White light emission from Tm³⁺/Dy³⁺ co-doped oxyfluoride germanate glasses under UV light excitation

G. Lakshminarayana, Hucheng Yang, Jianrong Qiu *

State Key Laboratory of Silicon Materials, Zhejiang University, Hangzhou 310027, China

ARTICLE INFO

ABSTRACT

In this paper, we report on the absorption and photoluminescence properties of Tm³⁺/Dy³⁺ ions co-doped oxyfluoride germanate glasses for white light emission. The X-ray diffraction (XRD) and differential thermal analysis (DTA) profiles of the host glass have been carried out to confirm its structure and thermal stability. From the measured absorption spectra, Judd–Ofelt (J–O) intensity parameters (Ω_2, Ω_4 and Ω_6) have been evaluated for Tm³⁺ and Dy³⁺ ions. A combination of blue, yellow and red emissions has emerged in these glasses, which allows the observation of bright white light when the glasses are excited by the ultraviolet light. The white light luminescence colour could be changed by varying the excitation wavelength. Also, various colours of luminescence, including white light, can be easily tuned by adjusting the concentrations of Tm³⁺ or Dy³⁺ ions in the co-doped glasses. Concentration quenching effect was also investigated and possible energy transfer mechanism from Dy³⁺→Tm³⁺ ions was explained which is also confirmed by the decay lifetime measurements.

© 2008 Elsevier Inc. All rights reserved.

1. Introduction

White light-emitting diodes (W-LEDs), the so-called next generation solid-state lighting (SSL) technology, are the current research focus in the lighting industry. White light LEDs show high potential for the replacement of conventional incandescent and fluorescent lamps due to the advantages of long lifetime, saving energy, reliability, safety and its environment-friendly characteristics [1–5]. The phosphor-converted (pc) emission method is common for creating white light with LEDs. White LEDs can be prepared by combining a gallium nitride (GaN)-based blue chip with yellow YAG:Ce³⁺ phosphor, in which a short wavelength blue light-emitting GaN-based LED is used to excite phosphors which emit yellow light and then mix the remaining blue light from the pump to compose desired white light. However, these white light LEDs based on blue LED plus yellow phosphor have low colour-rendering index R_a (CRI, in the 60–75 range), because of lack of red component in their spectra. As may be expected, red enhanced YAG:Ce or a small amount of red phosphor was introduced to improve the CRI to the acceptable range ($R_a > 80$) and increased the light conversion [6–8]. In addition to the blue LED plus yellow phosphor approach, three-band white LEDs were also proposed to achieve by the combination of the blue GaN-based LED with green and red phosphors, or the pumping of tri-colour (red, green and blue) phosphors with ultraviolet (UV) or violet LED. Three-band white LEDs maintain a very high colour-rendering index ($R_a > 90$) and were believed to offer the greatest potential for high efficiency solid-state lighting [9,10]. For excellent colour-rendering index, both methods need efficient red phosphors that should have the excitation wavelength matching with the emission wavelength of the blue LEDs ($\lambda_{em} = 440$–470 nm) or the UV/violet LEDs ($\lambda_{em} = 350$–420 nm). The presently used red phosphors for blue and near-UV/violet GaN-based LED are commercially still limited to divalent Eu ion-activated alkaline earth binary sulfides and Y₂O₂S:Eu³⁺, respectively. However, these sulfide-based phosphors are chemically unstable and the lifetimes of these materials are inadequate, and their luminescent intensities are very low relative to blue and green phosphors.

While majority of researches have focused on full-colour phosphors, glasses doped with rare-earth ions (REⁿ⁺) could be considered as an alternative approach due to advantages such as lower production cost, simpler manufacture procedure, free from halo effect and environment-friendly characteristics, etc. [11]. Recently, a zinc-aluminoborosilicate glass which emitted white light under UV light excitation by co-doping Eu₂O₃ and Dy₂O₃ [12] was reported. The white light emission was combined with multi-colour emission bands of Eu²⁺, Eu³⁺ and Dy³⁺ ions. However, the

* Corresponding author. Fax: +86 571 88925079.
E-mail address: qjr@zju.edu.cn (J. Qiu).

luminescence colour of the Eu–Dy ions co-doped glasses is strongly dependent on $Eu^{3+} \to Eu^{2+}$ reduction in air, and the reduction reaction would affect relative concentration of Eu^{2+} and Eu^{3+} ions significantly. Since many factors would affect the $Eu^{3+} \to Eu^{2+}$ reduction process in glass materials prepared in air, e.g. glass optical basicity, rigidity of glass network, valence of glass network modifier oxides, etc., the reaction was sensitive to glass compositions [13,14]. Since many fluorescent transitions of rare-earth ions of practical importance are initiated from an excited level with a small energy gap, materials with lower phonon energy are often required as a luminescent host to suppress the non-radiative loss and to obtain higher quantum efficiency of the desired fluorescence. However, most oxide glasses have large phonon energy ($1100\,cm^{-1}$) due to the stretching vibration of network-forming oxides. Fluoride glasses have an advantage due to their low phonon energy ($300–400\,cm^{-1}$) and higher quantum efficiency of many active transitions, but the stability and fiberizability as a practical material still remain problems. On the other hand, rare-earth ion-doped transparent oxyfluoride glasses have attracted great interest due to their excellent optical properties like fluoride glasses and good mechanical, chemical properties like oxide glasses. Recently, Shimin Liu et al. [15] has reported the white colour luminescence from Tm–Dy ions co-doped aluminoborosilicate glasses under UV light excitation. They reported a combination of blue, green, yellow, and red emission bands for white light emission under UV light excitation. We know that rare-earth ions will exhibit sharp emission or excitation bands in optical materials. But, the sharpness of these bands also depends on the host matrices phonon energies. It is a well-known fact that germanate glasses have smaller maximum vibrational frequencies than those shown by silicate, phosphate and borate glasses [16–19]. The maximum phonon energy of our selected oxyfluoride germanate host glass is around $740\,cm^{-1}$, which could be much lower than to the reported aluminoborosilicate glasses [15] for white light emission. Neto et al. [20] has reported white light emission in $Tm^{3+}/Ho^{3+}/Yb^{3+}$ triply doped fluorolead germanate glasses through upconversion route. RGB upconversion luminescence assigned to holmium and thulium ions both excited by means of successive energy tranfers from ytterbium ions was observed. White light was experimentally shown with the simultaneous generation of fluorescence with controllable intensities at the wavelengths of the three primary colours in a single sample and using a single near-infrared excitation source. Recently, Wang et al. [21,22] has also reported white light emission in transparent glass ceramics through upconversion route. By reasonably adjusting Yb^{3+}, Tm^{3+} and Er^{3+} contents, the intense red, green and blue emissions with almost equal intensity were obtained in the $0.5Yb^{3+}/0.1Tm^{3+}/0.05Er^{3+}$ triply doped glass ceramic, which yields the bright white light [21]. Also the red, green and blue signals, assigned to Ho^{3+} $^5F_5 \to {}^5I_8$, Ho^{3+} $^4S_2(^5F_4) \to {}^5I_8$ and Tm^{3+} $^1D_2 \to {}^3F_4$, $^1G_4 \to {}^3H_6$ transitions, respectively, were achieved via successive ET from Yb^{3+} to Ho^{3+} or Tm^{3+} for white light emission [22]. In the present work, we have reported the luminescence properties of oxyfluoride germanate glasses with Dy^{3+}/Tm^{3+} ions in terms of their unique feature of emitting white light under the UV excitation corresponding to the InGaN-based LED chip. The luminescence properties of these glasses are investigated by the absorption, emission and excitation spectra and their dependence on Tm^{3+} or Dy^{3+} concentration.

2. Experimental studies

Glasses with compositions of $50GeO_2–10B_2O_3–10ZnO–10Li_2O–20LaF_3$ (host glass) (mol%), $(50−x−y)GeO_2–10B_2O_3–10ZnO–10Li_2O–20LaF_3–xTm_2O_3–yDy_2O_3$ ($x = 1, y = 0$; $x = 0, y = 1$; $x = 1, y = 1$); $(50−x−y)GeO_2–10B_2O_3–10ZnO–10Li_2O–20LaF_3–xTm_2O_3–yDy_2O_3$ ($x = 0.25, y = 0.75$; $x = 0.5, y = 0.5$; $x = 0.75, y = 0.25$); and $(50−x−y)$ $GeO_2–10B_2O_3–10ZnO–10Li_2O–20LaF_3–xTm_2O_3–yDy_2O_3$ ($x = 0.25, y = 1.75$; $x = 0.5, y = 1.5$; $x = 0.75, y = 1.25$; $x = 1.25, y = .75$; $x = 1.5, y = 0.5$) were prepared by the conventional melt-quenching method. For convenience, in figures and CIE diagram we labeled $1.0Tm^{3+}$, $1.0Dy^{3+}$, $1.0Tm^{3+}/1.0Dy^{3+}$, $0.25Tm^{3+}/0.75Dy^{3+}$, $0.5Tm^{3+}/0.5Dy^{3+}$, $0.75Tm^{3+}/0.25Dy^{3+}$, $0.25Tm^{3+}/1.75Dy^{3+}$, $0.5Tm^{3+}/1.5Dy^{3+}$, $0.75Tm^{3+}/1.25Dy^{3+}$, $1.25Tm^{3+}/0.75Dy^{3+}$ and $1.5Tm^{3+}/0.5Dy^{3+}$ (mol%) co-doped glasses as (a), (b), (c), (d), (e), (f), (g), (h), (i), (j) and (k), respectively. We have also prepared $0.5Dy^{3+}$, $1.0Dy^{3+}$, $1.5Dy^{3+}$ and $2.0Dy^{3+}$ (mol%) glasses keeping $0.1\,mol\%Tm^{3+}$ as constant to study the Dy^{3+} ions concentration effect on Tm^{3+} ions. Reagents of GeO_2 (99.999%), H_3BO_3 (99.95%), ZnO (99.9%), Li_2CO_3 (99.99%), LaF_3 (99.99%), Tm_2O_3 (99.99%) and Dy_2O_3 (99.99%) were used as raw materials. Batches of 20 g were melted in a covered Pt–Rh crucible in air at $1250\,^\circ C$ for 30 min. and then the melt was cast onto a slab on a pre-heated iron plate. The quenched glasses were then annealed at $450\,^\circ C$ for 2 h, after which the annealing oven was turned off until the samples were finally cooled to the room temperature. Such prepared glasses are optically transparent. All of the samples were cut into $10 \times 10 \times 2\,mm^3$ size and polished for photoluminescence and absorption spectral measurements.

The densities of the glasses were measured using the buoyancy method based on the Archimedes principle with toluene as an immersion liquid. An Abbe refractometer was used to measure the refractive indices at Na (589.3 nm) lamp wavelength. Powder X-ray diffraction (XRD) spectrum was obtained on a Rigaku D/MAX-RA diffractometer with a Ni-filter and $CuK\alpha$ ($= 1.542\,\text{Å}$) radiation with an applied voltage of 340 kV and 20 mA anode current, calibrated with Si at the rate of $2\,^\circ C$/min. Differential thermal analysis (DTA) measurement was carried out on a SDT Q600 in the temperature range $30–1000\,^\circ C$, at the rate of $10\,^\circ C$/min, under N_2-gas atmosphere. Absorption spectra were recorded on a Hitachi U-4100, using a dual-beam spectrophotometer. The photoluminescence spectra were obtained on a Hitachi F-4500 with a 450W Xenon lamp as an excitation source. In order to compare the relative fluorescence intensity between the studied glasses, the conditions of excitation and detection systems were fixed, and the samples with the same shape were set at the same place in the experimental setup. On the basis of the signal-to-noise ratio, the relative errors in the spectral measurements are estimated to be $\pm 2\%$. The fluorescence decay curves were recorded by using a FLS920 fluorescence spectrophotometer. The temporal decay curves of the fluorescence signals were stored by using the attached storage digital oscilloscope. The relative error in the measurement of fluorescence lifetime is estimated to be $\pm 2\%$. For data fitting processes also, the error is $\pm 2\%$. Besides, systematic errors have been deducted through the standard instrument corrections. All the measurements were carried out at room temperature.

3. Results and discussion

Fig. 1 presents the XRD profile of the $50GeO_2–10B_2O_3–10ZnO–10Li_2O–20LaF_3$ glass, which confirms its amorphous structural nature with no sign of diffraction peaks. Fig. 2 presents the DTA thermogram of the host glass. From this profile, we have identified glass transition temperature (T_g, i.e., as determined by the inflection point at a temperature difference step change) at $535\,^\circ C$ and two crystallization peaks at $620\,^\circ C$ (T_{c1}) and $713\,^\circ C$ (T_{c2}). Thermal stability of glasses is a measure of disorder of glassy state. During the fiber fabrication process the preform will be
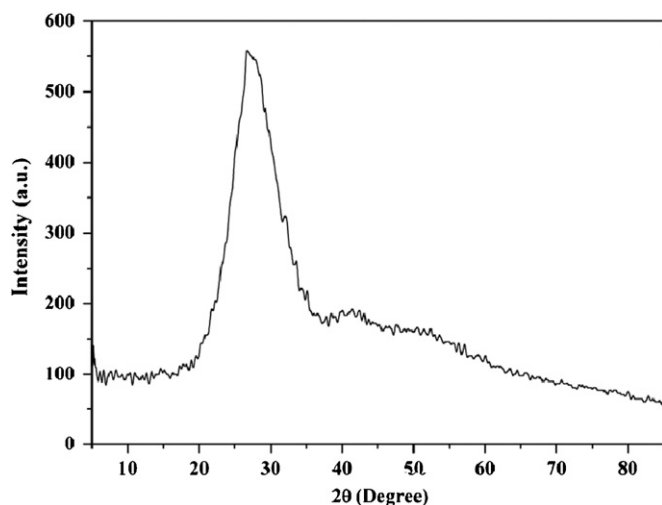
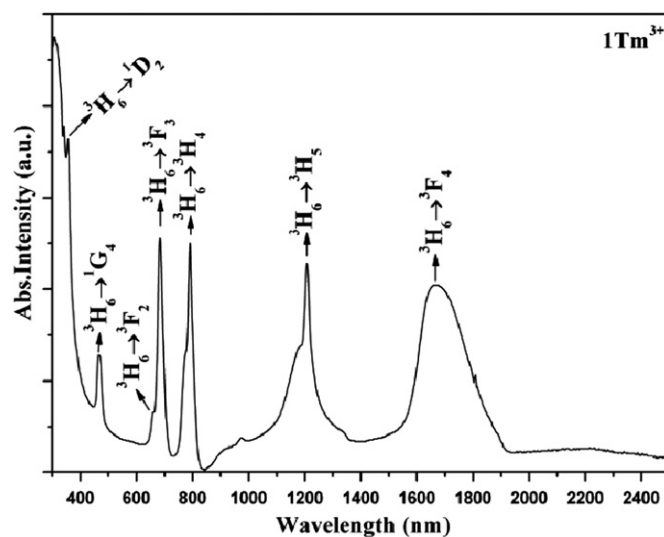**Fig. 1.** XRD profile of the $50GeO_2$–$10B_2O_3$–$10ZnO$–$10Li_2O$–$20LaF_3$ glass.

Fig. 3. Absorption spectrum of 1 mol%Tm^{3+}-doped glass.

Fig. 2. DTA profile of the $50GeO_2$–$10B_2O_3$–$10ZnO$–$10Li_2O$–$20LaF_3$ glass.

Table 1
Measured and calculated oscillator strengths ($f \times 10^{-6}$) and J–O intensity parameters of 1.0 mol% Tm^{3+} ions doped glass.

Wavelength (nm)	Energy (cm^{-1})	Transition	$\int \alpha \, d\lambda$ (10^{-7})	$f_{exp.}$ (10^{-6})	$f_{cal.}$ (10^{-6})
356	28089	$^1D_2$	42.72638	15.1352	14.23341
466	21459	$^1G_4$	21.24115	4.78931	3.94059
683	14641	$^3F_3$	121.12787	11.2105	12.13352
792	12626	$^3H_4$	130.75253	8.087	6.63421
1207	8285	$^3H_5$	189.31981	5.36276	5.21362
1666	6002	$^3F_4$	523.10362	8.47391	10.38514

$\Omega_2 = 8.814 \times 10^{-20} \, cm^2$, $\Omega_4 = 13.231 \times 10^{-20} \, cm^2$, $\Omega_6 = 3.102 \times 10^{-20} \, cm^2$.

relation:

$$f_{exp} = 4.318 \times 10^{-9} \int \varepsilon(\upsilon) \, d\upsilon \qquad (1)$$

where $\varepsilon(\upsilon)$ is the molar extinction coefficient at average energy (υ) in cm^{-1}. The experimental oscillator strengths of absorption bands of Tm^{3+}-doped glass is determined with the known values of the Tm^{3+} concentration, sample thickness, peak position and peak areas by using Eq. (1). We have applied least-square fitting procedure to determine the J–O intensity parameters Ω_2, Ω_4 and Ω_6 [24,25] by using the experimentally measured oscillator strengths and the obtained values are presented in Table 1. Fig. 4 presents the absorption spectrum of 1 mol%Dy^{3+}-doped glass. The bands are assigned from the ground state, $^6H_{15/2}$. The transitions from the next excited state $^6H_{13/2}$ may be ruled out due to thermalization as the energy gap between $^6H_{15/2}$ and $^6H_{13/2}$ is around 3000 cm^{-1}. From this spectrum, the levels of $^4M_{15/2}$, $^6P_{7/2}$ (350 nm), $^4I_{11/2}$ (364 nm), $^4I_{13/2}$, $^4F_{7/2}$ (387 nm), $^4G_{11/2}$ (428 nm), $^4I_{15/2}$ (451 nm), $^6F_{3/2}$ (749 nm), $^6F_{5/2}$ (799 nm), $^6F_{7/2}$ (897 nm), ($^6H_{7/2}$, $^6F_{9/2}$) (1086 nm), ($^6F_{11/2}$, $^6H_{9/2}$) (1266 nm) and $^6H_{11/2}$ (1672 nm) are well resolved [23]. In the case of Dy^{3+} ($4f^9$) ion, the hypersensitive transition ($^6F_{11/2}$, $^6H_{9/2}$) is found to be more intense than the other transitions [26]. From these observed absorption bands we have calculated the J–O intensity parameters and the results are presented in Table 2.

Fig. 5 shows the absorption spectra of (a) 1Tm^{3+}, 1Dy^{3+} and 1Dy^{3+}/1Tm^{3+} (mol%), (b) 0.25Tm^{3+}/0.75Dy^{3+}, 0.5Tm^{3+}/0.5Dy^{3+} and 0.75Tm^{3+}/0.25Dy^{3+}, (c) 0.25Tm^{3+}/1.75Dy^{3+}, 0.5Tm^{3+}/1.5Dy^{3+},

subjected to various heating cycles above T_g. If the glass has a poor thermal stability, then crystallization could occur in the glass during the heating cycles. The crystals thus formed will scatter the input signals and contribute to attenuation rather than amplification. Thus, evaluation of thermal stability of glass is important to examine its suitability as an optical fiber.

Fig. 3 shows the absorption spectrum of 1 mol%Tm^{3+}-doped glass. The rare-earth ions are characterized by partially filled $4f$ shell which is shielded by $5s^2$ and $5p^6$ electrons. All transitions in the absorption spectrum of Tm^{3+} start from the ground state $^3H_6$ to the various excited states. The transitions observed in the absorption spectrum of Tm^{3+} are intra-configurational (f–f) transitions with almost absence of overlapping with the surrounding ions. The spectrum is characterized by seven bands corresponding to the transitions starting from the $^3H_6$ ground state to the different higher levels $^1D_2$ (356 nm), $^1G_4$ (466 nm), $^3F_2$ (656 nm), $^3F_3$ (683 nm), $^3H_4$ (792 nm), $^3H_5$ (1207 nm) and $^3F_4$ (1666 nm) [23]. The absorption bands measured are all dominated by electric-dipole transitions except the transition $^3H_6 \rightarrow ^3H_5$, which contains electric-dipole and magnetic-dipole contributions. The experimental oscillator strengths (f) of the absorption spectral transitions of Tm^{3+} ions doped glass are calculated using the

Fig. 4. Absorption spectrum of 1 mol%Dy^{3+}-doped glass.

Table 2
Measured and calculated oscillator strengths ($f \times 10^{-6}$) and J–O intensity parameters of 1.0 mol% Dy^{3+} ions doped glass.

Wavelength (nm)	Energy (cm^{-1})	Transition	$f_{exp.}$ (10^{-6})	$F_{cal.}$ (10^{-6})
799	12515.644	$^6F_{5/2}$	0.353068	0.393998
897	11148.272	$^6F_{7/2}$	0.657722	0.737555
1086	9208.103	$^6F_{7/2}+^6F_{9/2}$	0.720874	0.732789
1266	7898.9	$^6H_{9/2}+^6F_{11/2}$	3.67809	3.819771
1672	5980.86	$^6H_{11/2}$	0.731598	0.5630004

0.75Tm^{3+}/1.25Dy^{3+}, 1.25Tm^{3+}/0.75Dy^{3+} and 1.50Tm^{3+}/0.5Dy^{3+} co-doped glasses from 300 to 700 nm wavelength. From 1 mol%Tm^{3+}-doped glass, absorption bands centered at 356 nm ($^3H_6 \rightarrow {}^1D_2$), 466 nm ($^3H_6 \rightarrow {}^1G_4$), 656 nm ($^3H_6 \rightarrow {}^3F_2$) and 683 nm ($^3H_6 \rightarrow {}^3F_3$) are observed. From 1 mol%Dy^{3+}-doped glass, absorption bands at 350 nm ($^6H_{15/2} \rightarrow {}^4M_{15/2}$, $^6P_{7/2}$), 364 nm ($^6H_{15/2} \rightarrow {}^4I_{11/2}$), 387 nm ($^6H_{15/2} \rightarrow {}^4I_{13/2}$, $^4F_{7/2}$), 428 nm ($^6H_{15/2} \rightarrow {}^4G_{11/2}$) and 451 nm ($^6H_{15/2} \rightarrow {}^4I_{15/2}$) are observed. Absorption spectra of all the co-doped glasses show the similar characteristics, although they are doped with different Tm^{3+}/Dy^{3+} ions concentration. For Tm^{3+}/Dy^{3+} co-doped glasses, all of the absorption bands referred above are presented. Moreover, in all co-doped glasses the absorption band centered at 350 nm could be assigned to the overlapping of Tm^{3+}:$^3H_6 \rightarrow {}^1D_2$ and Dy^{3+}:$^6H_{15/2} \rightarrow {}^4M_{15/2}$, $^6P_{7/2}$ transitions. In all co-doped glasses, the absorption band intensity centered at 683 nm ($^3H_6 \rightarrow {}^3F_2$) is considerably increased with Tm^{3+} concentration increment.

Fig. 6 shows the excitation spectra of (a) 1Dy^{3+}/1Tm^{3+} (mol%), (b) 0.25Tm^{3+}/0.75Dy^{3+}, 0.5Tm^{3+}/0.5Dy^{3+} and 0.75Tm^{3+}/0.25Dy^{3+}, (c) 0.25Tm^{3+}/1.75Dy^{3+}, 0.5Tm^{3+}/1.5Dy^{3+}, 0.75Tm^{3+}/1.25Dy^{3+}, 1.25Tm^{3+}/0.75Dy^{3+} and 1.50Tm^{3+}/0.5Dy^{3+} co-doped glasses monitoring emissions at 455, 482 and 575 nm, respectively. The excitation spectra of all the Tm^{3+}/Dy^{3+} co-doped glasses exhibit the similar characteristics. From 1Tm^{3+}/1Dy^{3+} (mol%) co-doped glass, excitation bands centered at 325 nm ($^6H_{15/2} \rightarrow {}^4M_{17/2}$), 350 nm ($^4M_{15/2}$, $^6P_{7/2}$), 364 nm ($^6H_{15/2} \rightarrow {}^4I_{11/2}$), 386 nm ($^6H_{15/2} \rightarrow {}^4I_{13/2}$, $^4F_{7/2}$), and 425 nm ($^6H_{15/2} \rightarrow {}^4G_{11/2}$), 452 nm ($^6H_{15/2} \rightarrow {}^4I_{15/2}$) and 472 nm ($^6H_{15/2} \rightarrow {}^4F_{9/2}$) are observed by monitoring emission at 575 nm. Besides, the observed excitation band centered at 350 nm by monitoring emissions at 482 and 575 nm corresponds to the $^3H_6 \rightarrow {}^1D_2$ electronic transition of Tm^{3+} ions. From these spectra, it is observed that all the oxyfluoride germanate glasses

Fig. 5. Absorption spectra of (a) 1Tm^{3+}, 1Dy^{3+} and 1Dy^{3+}/1Tm^{3+} (mol%), (b) 0.25Tm^{3+}/0.75Dy^{3+}, 0.5Tm^{3+}/0.5Dy^{3+}, 0.75Tm^{3+}/0.25Dy^{3+} (mol%), (c) 0.25Tm^{3+}/1.75Dy^{3+}, 0.5Tm^{3+}/1.5Dy^{3+}, 0.75Tm^{3+}/1.25Dy^{3+}, 1.25Tm^{3+}/0.75Dy^{3+} and 1.50Tm^{3+}/0.5Dy^{3+} (mol%) co-doped glasses.

Fig. 6. Excitation spectra of (a) 1Dy^{3+}/1Tm^{3+} (mol%), (b) 0.25Tm^{3+}/0.75Dy^{3+}, 0.5Tm^{3+}/0.5Dy^{3+} and 0.75Tm^{3+}/0.25Dy^{3+}, (c) 0.25Tm^{3+}/1.75Dy^{3+}, 0.5Tm^{3+}/1.5Dy^{3+}, 0.75Tm^{3+}/1.25Dy^{3+}, 1.25Tm^{3+}/0.75Dy^{3+} and 1.50Tm^{3+}/0.5Dy^{3+} co-doped glasses monitoring emissions at 455, 482 and 575 nm, respectively.

could be efficiently excited by UV radiation. Also the emission intensity of Tm^{3+}/Dy^{3+} ions co-doped glasses can be adjusted by changing the excitation light, and the luminescence colour could be adjusted. Interestingly, an overlapped excitation bands from
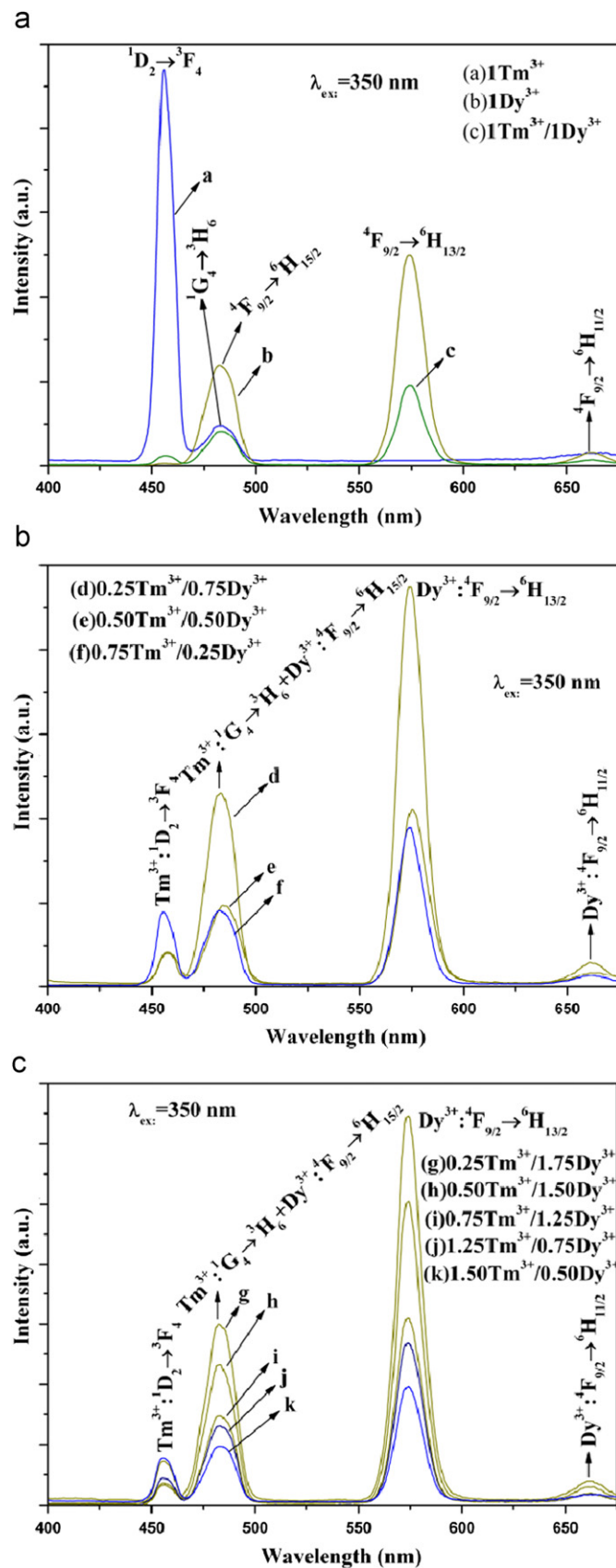
Fig. 7. Emission spectra of (a) 1Tm^{3+}, 1Dy^{3+} and 1Dy^{3+}/1Tm^{3+} (mol%), (b) 0.25Tm^{3+}/0.75Dy^{3+}, 0.5Tm^{3+}/0.5Dy^{3+} and 0.75Tm^{3+}/0.25Dy^{3+}, (c) 0.25Tm^{3+}/1.75Dy^{3+}, 0.5Tm^{3+}/1.5Dy^{3+}, 0.75Tm^{3+}/1.25Dy^{3+}, 1.25Tm^{3+}/0.75Dy^{3+} and 1.50Tm^{3+}/0.50Dy^{3+} co-doped glasses with 350 nm excitation wavelength.

340 to 370 nm are observed for all the Tm^{3+}/Dy^{3+} ions co-doped glasses, monitoring emissions at 455, 482 and 575 nm, respectively. It indicates that the blue and yellow emission bands referred above can be excited by UV light simultaneously in the Tm^{3+}/Dy^{3+} co-doped glasses. Considering the synchronous emissions of these two ions, it is believed that the appropriate excitation wavelength is at about 350 nm, which fits to the requirements of W-LED.

Fig. 7 shows the emission spectra of (a) $1Tm^{3+}$, $1Dy^{3+}$ and $1Dy^{3+}/1Tm^{3+}$ (mol%), (b) $0.25Tm^{3+}/0.75Dy^{3+}$, $0.5Tm^{3+}/0.5Dy^{3+}$ and $0.75Tm^{3+}/0.25Dy^{3+}$, (c) $0.25Tm^{3+}/1.75Dy^{3+}$, $0.5Tm^{3+}/1.5Dy^{3+}$, $0.75Tm^{3+}/1.25Dy^{3+}$, $1.25Tm^{3+}/0.75Dy^{3+}$ and $1.50Tm^{3+}/0.5Dy^{3+}$ co-doped glasses with 350 nm excitation wavelength. From $1 mol\%Tm^{3+}$-doped glass, strong emission band centered at 455 nm ($^1D_2 \rightarrow {}^3F_4$) and another small band centered at 482 nm ($^1G_4 \rightarrow {}^3H_6$) are observed. For $1 mol\%Dy^{3+}$-doped glass, strong emission bands at $^4F_{9/2} \rightarrow {}^6H_{15/2}$ (482 nm) and $^4F_{9/2} \rightarrow {}^6H_{13/2}$ (575 nm) and a weak emission band at $^4F_{9/2} \rightarrow {}^6H_{11/2}$ (662 nm), respectively, are observed. Among these, the transition $^4F_{9/2} \rightarrow {}^6H_{13/2}$ has shown bright yellow emission intensity, i.e. a major part of the emission intensity is contained in the $^4F_{9/2} \rightarrow {}^6H_{13/2}$ transition. For all Tm^{3+}/Dy^{3+} co-doped glasses, all of the emission bands referred above are identified in their emission spectra under 350 nm excitation wavelength. But the existence of the emission band of $^1G_4 \rightarrow {}^3H_6$ for Tm^{3+} at 482 nm is uncertain, because it may be overlapped by the strong emission band of $^4F_{9/2} \rightarrow {}^6H_{15/2}$ of Dy^{3+} ions at 482 nm. Most strikingly, the intensity of blue, yellow and red emissions of Dy^{3+} ions decreases with the increasing Tm^{3+} concentration, which indicates a potential energy transfer from Dy^{3+} ions to Tm^{3+}ions. From the absorption spectra, it is observed that there is a broad absorption band from 460 to 480 nm in all the Dy^{3+}/Tm^{3+} co-doped glasses due to Tm^{3+} ($^3H_6 \rightarrow {}^1G_4$), which overlaps with the blue emission band of Dy^{3+} (465–495 nm). That is, emission at 455 nm from Tm^{3+} ion could be enhanced at the cost of the blue emission intensity of Dy^{3+} in all the co-doped glasses. So, there is a possibility of tuning the chromaticity parameters of the present glasses by varying the concentration of Tm^{3+} or Dy^{3+} ions. This is very important for lighting applications where the chromaticity coordinate's characterization in the CIE chromaticity diagram is indispensable.

Fig. 8 presents the decay curves of (a) $1Tm^{3+}$, $1Tm^{3+}/1Dy^{3+}$ (mol%), (b) $0.25Tm^{3+}/0.75Dy^{3+}$, $0.75Tm^{3+}/0.25Dy^{3+}$ (mol%), (c) $0.25Tm^{3+}/1.75Dy^{3+}$, $1.5Tm^{3+}/0.5Dy^{3+}$ (mol%) co-doped glasses. When the interaction between luminescent ions is not important, the decay of the luminescence can be fitted to a single exponential. However, when the ions concentration is large enough, energy transfer appears and the decay curves become nonexponential. From all these decay curves, it is clearly observed that with increasing Tm^{3+} concentration in all the co-doped glasses the lifetimes of blue (482 nm) and yellow (575 nm) emission bands of Dy^{3+} ions are decreased while the lifetime of blue (455 nm) emission band of Tm^{3+} is increased. From these decay lifetime measurements, the energy transfer from Dy^{3+} to Tm^{3+} is confirmed. Luminescence colours of all the glasses, i.e. from (a) to (k) excited at 350 nm are characterized by CIE chromaticity diagram and shown in Fig. 9(a). It shows that blue and yellowish white light can be observed in single Tm^{3+} and Dy^{3+}-doped glasses, respectively. Since white light can be synthesized by appropriate combination of blue and yellow light, the typical white light emission can be achieved in Tm^{3+}/Dy^{3+} co-doped oxyfluoride germanate glasses, as shown in Fig. 9(a). Fig. 9(b) shows the enlarged spectrum for colour coordinate (X) value from 0.33 to 0.37. We also investigated the effect of Dy^{3+} ion concentration on Tm^{3+} ions. We kept Tm^{3+} ion concentration at 0.1 mol% and Dy^{3+} ion concentration is varied from 0.5 to 2.0 mol%.
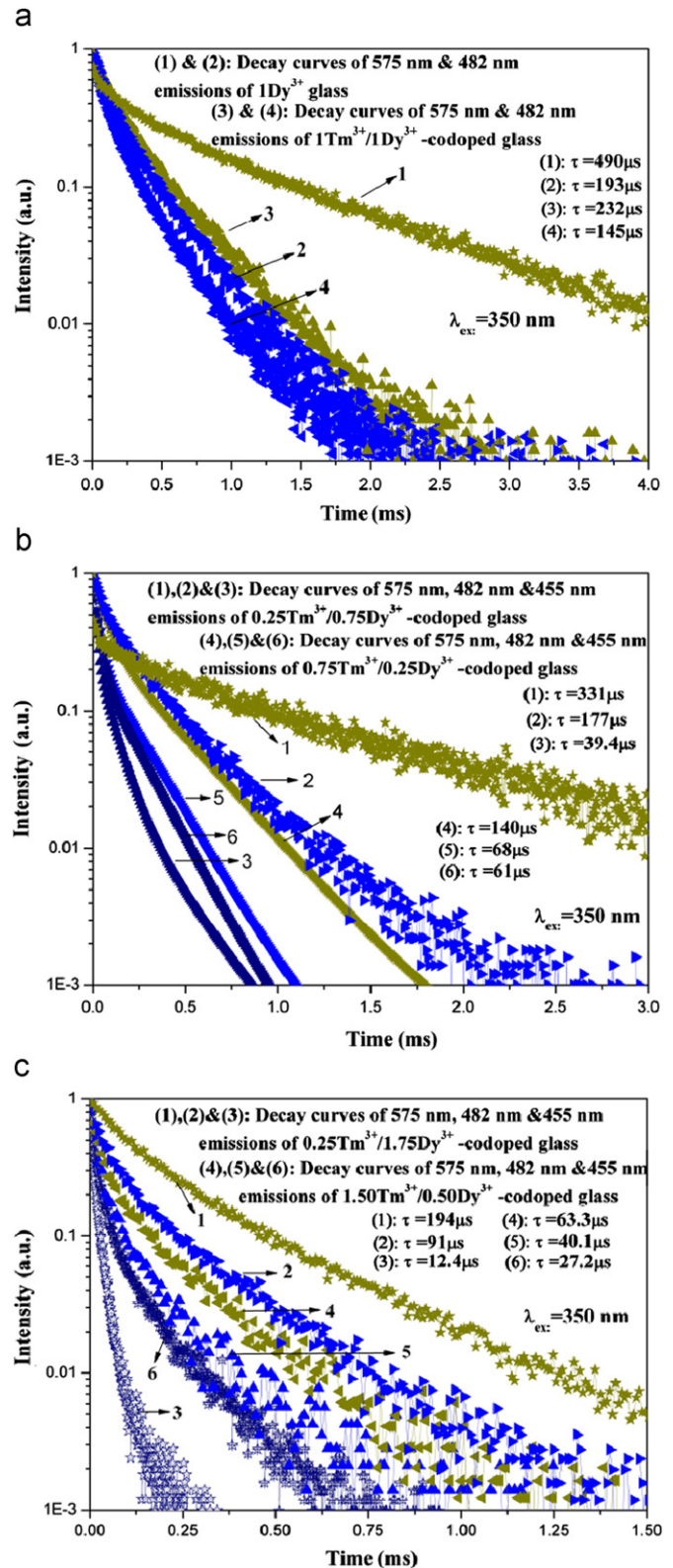

Fig. 8. Decay curves of (a) $1Tm^{3+}$, $1Tm^{3+}/1Dy^{3+}$ (mol%), (b) $0.25Tm^{3+}/0.75Dy^{3+}$, $0.75Tm^{3+}/0.25Dy^{3+}$(mol%), (c) $0.25Tm^{3+}/1.75Dy^{3+}$, $1.5Tm^{3+}/0.5Dy^{3+}$(mol%) co-doped glasses (Y-axis on semilog scale).

Fig. 10 presents the emission spectra of the $0.5Dy^{3+}$, $1.0Dy^{3+}$, $1.5Dy^{3+}$ and $2.0Dy^{3+}$ (mol%) glasses co-doped with $0.1 mol\%Tm^{3+}$ concentration under 350 nm excitation wavelength. From these spectra, four emission bands centered at 455 nm (Tm^{3+}: $^1D_2 \rightarrow {}^3F_4$),
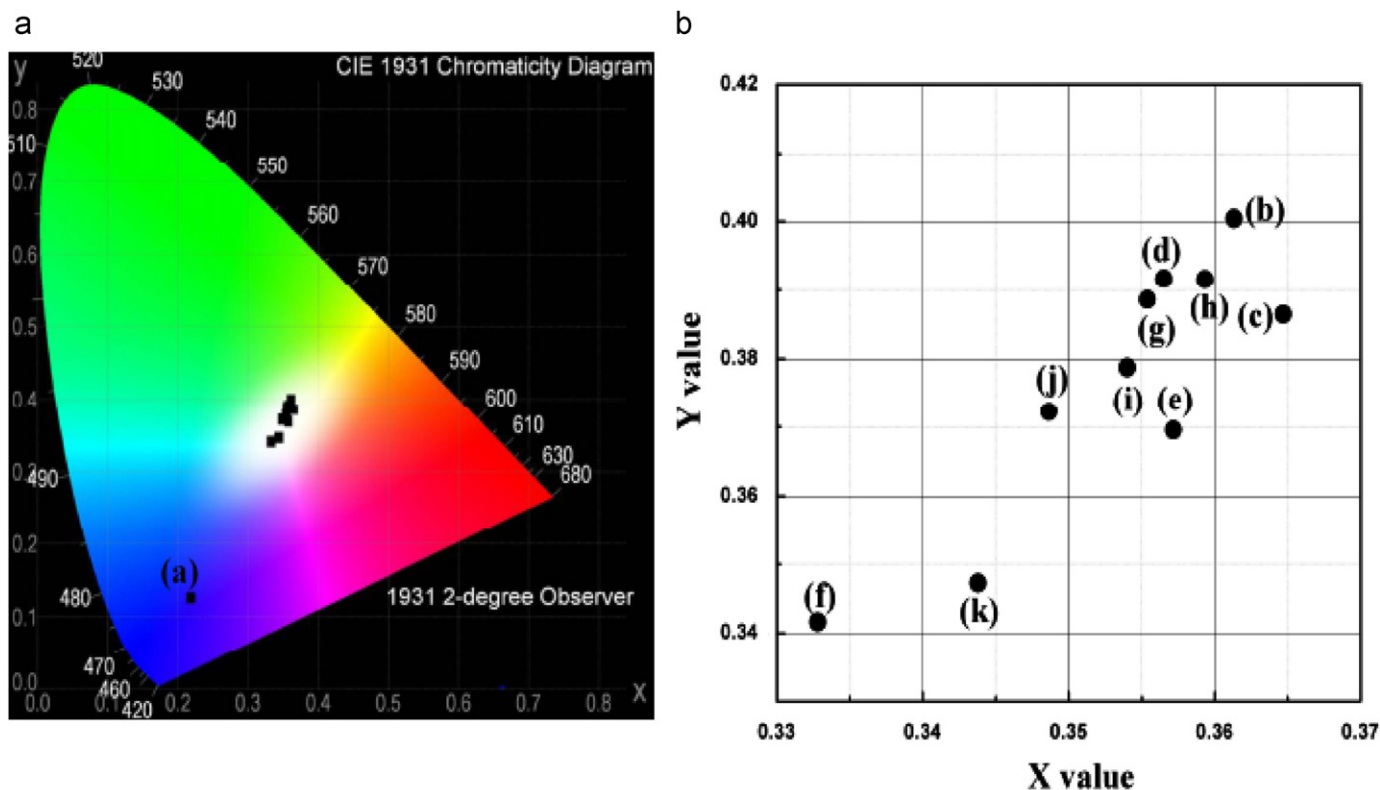
a

b

Fig. 9. (a) Cromaticity diagram for all the studied, i.e. ((a)–(k)) Tm^{3+}/Dy^{3+} co-doped glasses. (b) Enlarged spectrum for colour coordinate (X) value from 0.33 to 0.37.

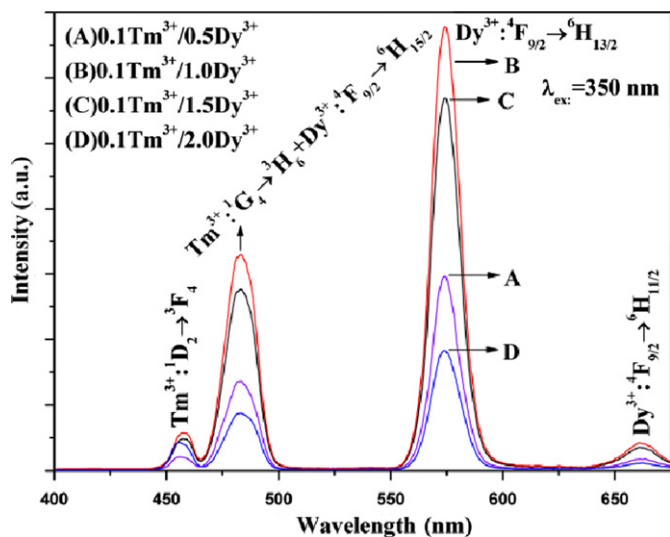**Fig. 10.** Emission spectra of $0.5Dy^{3+}$, $1.0Dy^{3+}$, $1.5Dy^{3+}$ and $2.0Dy^{3+}$ (mol%) glasses co-doped with $0.1 \, mol\% Tm^{3+}$ concentration under 350 nm excitation wavelength.

482 nm ($Tm^{3+}:^{1}G_{4} \rightarrow {}^{3}H_{6}+Dy^{3+}:^{4}F_{9/2} \rightarrow {}^{6}H_{15/2}$), 575 nm ($Dy^{3+}:^{4}F_{9/2} \rightarrow {}^{6}H_{13/2}$) and 662 nm ($Dy^{3+}:^{4}F_{9/2} \rightarrow {}^{6}H_{11/2}$) are observed. It is observed that from 0.5 to 1.0 mol%Dy^{3+}, the intensity of luminescence bands of Tm^{3+} and Dy^{3+} increased and above 1 mol%Dy^{3+} concentration, their intensities are decreased due to concentration quenching.

Based on the emission, excitation spectra and decay lifetime measurements, the energy transfer process from Dy^{3+} to Tm^{3+} ions in co-doped oxyfluoride germanate glasses is described in the energy level scheme, as shown in Fig. 11. Two non-radiative transition processes of $^{1}D_{2} \rightarrow {}^{1}G_{4}$ for Tm^{3+} ion and $^{4}M_{15/2}$, $^{6}P_{7/2}$
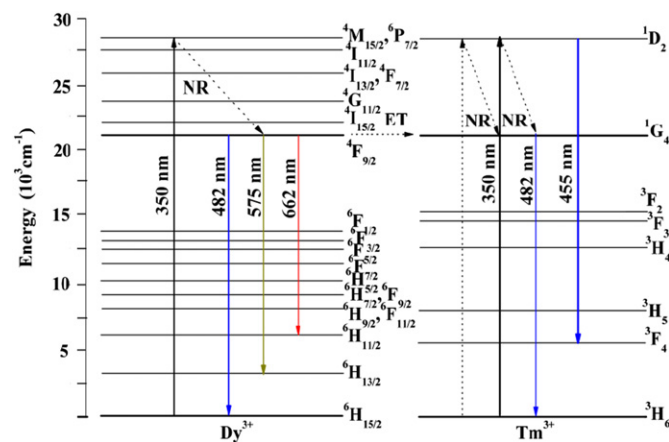

Fig. 11. Energy level scheme for energy transfer process between Dy^{3+} and Tm^{3+} ions in studied glasses.

$\rightarrow {}^{4}F_{9/2}$ for Dy^{3+} ion are indicated in the energy level scheme. An assumption is employed here that the Dy^{3+} to Tm^{3+} energy transfer process can be enhanced if the rare-earth ions are not well separated in co-doped glass matrices. In other words, if Tm^{3+} and Dy^{3+} ions cluster together in the co-doped glass matrices then the probability of energy transfer process from Dy^{3+} to Tm^{3+} ions will increase. Thereby, it is possible to realize the generation of white light emission under UV light.

4. Conclusions

In summary, Tm^{3+} and Dy^{3+} ions co-doped oxyfluoride germanate glasses were successfully synthesized by the

melt-quenching method. Absorption and excitation spectra have shown that all these glasses can be effectively excited by UV light. Emission spectra have shown three emissions (482, 575 and 662 nm) for Dy^{3+}-doped glass and four emissions (455, 482 and 575 and 662 nm) for glasses co-doped with Tm^{3+} and Dy^{3+}. A typical white luminescence was observed in all the Tm^{3+}/Dy^{3+} co-doped glasses under 350 nm excitation. Energy transfer from Dy^{3+} to Tm^{3+} is also observed, with constant Tm^{3+} concentration. The intensity ratio of yellow to blue emissions can be tuned by varying the concentrations of both Tm^{3+} and Dy^{3+} ions. Thereby, it is possible to realize the generation of white light emission under UV light. Such efficient white light emission of the Tm^{3+}/Dy^{3+} co-doped glasses makes them as excellent candidates applicable in the solid-state multi-colour three-dimensional display.

Acknowledgments

References

[1] A.H. Mueller, M.A. Petruska, M. Achermann, D.J. Werder, E.A. Akhadov, D.D. Koleske, M.A. Hoffbauer, V.I. Klimov, Nanoletters 5 (6) (2005) 1039–1044.
[2] N. Narendran, Y. Gu, J.P. Freyssinier-Nova, Y. Zhu, Phys. Status Solidi (a) 202 (6) (2005) R60–R62.
[3] Y.Q. Li, A.C. Delsing, G. de With, H.T. Hintzen, Chem. Mater. 17 (2005) 3242–3248.
[4] M.S. Shur, A. Zukauskas, Solid state lighting: toward superior illumination, Proc. IEEE 93 (10) (2005) 1073–1691.
[5] M.J. Bowers ll, J.R. McBride, S.J. Rosenthal, J. Am. Chem. Soc. 127 (2005) 15378–15379.
[6] C.J. Summers, B. Wagner, H. Menkara, Solid state lighting: diode phosphors, Proc. SPIE 5187 (2004) 123–132.
[7] D.A. Steigerwald, J.C. Bhat, D. Collins, R.M. Fletcher, M.O. Holcomb, M.J. Ludowise, P.S. Martin, S.L. Rudaz, Illumination with solid state lighting technology, IEEE J. Sel. Top. Quantum Electron. 8 (2) (2002) 310–320.
[8] C.-H. Chiu, C.-H. Liu, S.-B. Huang, T.-M. Chen, J. Electrochem. Soc. 154 (7) (2007) J181–J184.
[9] T. Nishida, T. Ban, N. Kobayashi, Appl. Phys. Lett. 82 (22) (2003) 3817–4319.
[10] H. Wu, X. Zhang, C. Guo, J. Xu, M. Wu, Q. Su, IEEE Photonics Technol. Lett. 17 (6) (2005) 1160–1162.
[11] X. Liang, C. Zhu, Y. Yang, S. Yuan, G. Chen, J. Lumin. 128 (2008) 1162–1164.
[12] S. Liu, G. Zhao, H. Ying, J. Wang, G. Han, Opt. Mater. 31 (1) (2008) 47.
[13] C. Wang, M. Peng, N. Jiang, X. Jiang, C. Zhao, J. Qiu, Mater. Lett. 61 (2007) 3608.
[14] C. Zhu, Y. Yang, X. Liang, S. Yuan, G. Chen, J. Am. Ceram. Soc. 90 (2007) 2984.
[15] Shimin Liu, Gaoling Zhao, Xiaohua Lin, Hao Ying, Junbo Liu, Jianxun Wang, Gaorong Han, J. Solid State Chem. (2008).
[16] R. Balda, J. Fernaˊndez, A. de Pablos, J.M. Fdez-Navarro, J. Phys. Condens. Mater. 11 (38) (1999) 411.
[17] Z. Pan, S.H. Morgan, A. Loper, V. King, B.H. Long, W.E. Collins, J. Appl. Phys. 77 (9) (1995) 4688.
[18] M. Wachtler, A. Speghini, S. Pigorini, R. Rolli, M. Bettinelli, J. Non-Cryst. Solids 217 (1) (1997) 111.
[19] S.J.L. Ribeiro, J. Dexpert-Ghys, B. Piriou, V.R. Mastelaro, J. Non-Cryst. Solids 159 (1993) 213.
[20] S. Gouveia-Neto, L.A. Bueno, R.F. do Nascimento, E.A. da Silva Jr., E.B. da Costa, V.B. do Nascimento, Appl. Phys. Lett. 91 (2007) 091114.
[21] Daqin Chen, Yuansheng Wang, Kelu Zheng, Tailiang Guo, Yunlong Yu, Ping Huang, Appl. Phys. Lett. 91 (2007) 251903.
[22] A. Daqin Chen, A. Yuansheng Wang, A. Yunlong Yu, A. Ping Huang, A. Fangyi Weng, J. Solid State Chem. (2008).
[23] W.T. Carnall, P.R. Fields, K. Rajnak, J. Chem. Phys. 49 (1968) 4452.
[24] B.R. Judd, Phys. Rev. 127 (1962) 750.
[25] G.S. Ofelt, J. Chem. Phys. 37 (1962) 511.
[26] C.K. Jorgensen, B.R. Judd, Mol. Phys. 8 (1964) 281.